31st Congress of the International Council of the Aeronautical Sciences

Belo Horizonte, Brazil; September 09-14, 2018

VISCOUS FLUID SIMULATION WITH THE VORTEX ELEMENT METHOD

O.S. Kotsur* , **G.A. Shcheglov***

***Bauman Moscow State Technical University, Russia**

Keywords: *vortex methods, viscosity, particle strength exchange, PSE, diffusion velocity*

Abstract

Vortex methods has shown their effectiveness for several kinds of incompressible fluid dynamics problems, were the viscosity effects can be neglected. However simulation of viscous flows via vortex methods meets difficulties because of the viscosity term in the vorticity evolution equation that needs to be resolved.

In this paper we give a general overview of several viscosity models that we apply to the Vortex Element Method based on fragmentons. We consider three different approaches: Particle Strength Exchange, Diffusion Velocity Method and a hybrid scheme to approximate the viscosity term.

Finally, we show two simple simulation examples of the diffusion of rectilinear vortex and vortex ring in viscous fluid.

1 Introduction

Vortex Methods (VM) are a Computational Fluid Dynamics (CFD) tool used for resolving incompressible fluid dynamics problems [1]. VM being lagrangian methods, might be an alternative to conventional CFD mesh methods for external aero- and hydrodynamics problems [2, 3]. VM can be especially effective for Fluid-Structure Interaction (FSI) problems [4, 5], where mesh methods may have difficulties with handling moving boundaries because of the need to adapt the mesh on the boundary position every time step [6], or use special multiple-mesh technics (CHIMERA). Simulation of FSI problems with these kind of methods may lead to significant computational and time costs, which would not be the case for VM.

Let us consider the three-dimensional momentum equation for incompressible viscous fluid in boundless space

$$\frac{\partial \boldsymbol{\omega}}{\partial t} + (\boldsymbol{V}\cdot\nabla)\,\boldsymbol{\omega} = (\boldsymbol{\omega}\cdot\nabla)\,\boldsymbol{V} + \nu\Delta\boldsymbol{\omega} \qquad (1)$$

where $\boldsymbol{V} = \boldsymbol{V}(\boldsymbol{x},t)$, $\boldsymbol{\omega} = \nabla\times\boldsymbol{V}$ are velocity and vorticity fields respectively, $t\in[0,T]$; ν – kinematic viscosity.

Basically, vortex methods consist in approximation of the continuous vorticity field $\boldsymbol{\omega}$ with the superposition of a finite number of Vortex Elements (VE) $\boldsymbol{\omega}_k$. As a result, (1) can be rewritten as series of ODEs describing the evolution of each vortex particle (see section 2). In the case of ideal fluid VEs follow the trajectories of fluid particles.

Though VM are mostly based on Kelvin's Theorems that describe the dynamics of vorticity in ideal flow, lots of attempts have been made to extend the applicability of the VMs to viscous flows. As a result, several approaches have appeared to treat the viscosity term in the vorticity evolution equation. Here we consider three of them:

- Particle Strength Exchange (PSE) uses the approximation of the diffusion term $\nu\Delta\boldsymbol{\omega}$ with the integral operator of the specific form [1, 7].
- In the Diffusion Velocity Method (DVM) for viscous flows vortex particles follow

special trajectories defined by the so called 'diffusion velocity' and conserve their intensities unchanged [8, 9]. DVM is based on the reformulation of (1) in the convective form, which can be effectively resolved with the existing classical vortex methods. Works only for 2D and axisymmetric flows.

- To overcome this issue for general flows a special hybrid DVM-PSE approach was proposed by Mycek in [10]. The basic idea is to extract from the diffusion term $\nu\Delta\boldsymbol{\omega}$ the dominating part that can be treated with DVM, while the remaining part to be resolved with the PSE-approximation.

2 Vortex Element Method for ideal fluid

Consider a flow of ideal fluid with nonzero vorticity $\boldsymbol{\omega}$. We approximate $\boldsymbol{\omega}(\boldsymbol{x},t)$ a superposition of vortex element basis functions $\boldsymbol{\omega}_k(t)$:

$$\boldsymbol{\omega}(\boldsymbol{x},t) \approx \sum_{k=1}^{N} \boldsymbol{\omega}_k(\boldsymbol{x}-\boldsymbol{x}_k) \tag{2}$$

where $\boldsymbol{x}_k = \boldsymbol{x}_k(t)$ is the k-th VE marker position.

The choice of a basis function can significantly influence on the quality of the approximated vorticity field. First, the vorticity field is always solenoidal and we normally want it to vanish at infinity. Therefore, a good basis function should satisfy these constraints. Also, if a basis function is somehow 'adapted' to the structure of vorticity field, this would also benefit in approximation quality and in reducing the required number of VE to simulate the flow.

The classical, well known and the most commonly used model of VE is a singular point δ-function, called 'vorton' [1]

$$\boldsymbol{\omega}_k(\boldsymbol{x},t) = \alpha_k \delta(\boldsymbol{x}-\boldsymbol{x}_k) \tag{3}$$

where $\alpha_k = \alpha_k(t)$ is vector coefficient, which describes intensity and orientation of the vorton.

Singular point vorton (3) constitutes, basically, the classical particle approximation of the vorticity evolution equation (1). In the studies [11] reader can find a complete theoretical analysis of the vortex method based on vortons, namely, its convergence towards the solutions of Euler equations for incompressible fluid.

However, vorton (3) has two principle problems:

- (3) violates the solenoidity of the approximated vorticity field; [1];
- vorton model denotes amount of vorticity, concentrated in a singular point. If we look at the vorticity field as at the set of vortex lines, then it becomes clear that the use of 'vector particles' is not the best choice to approximate vortex lines.

We consider from now the so called 'fragmenton' model for the vortex element basis function (fig. 1). Fragmenton can be considered as a fragment of a vortex line. Its basis function is obtained by integration of the singular pointwise vorton (3) along the vector $2\boldsymbol{h}_k$, which can change its length and direction:

$$\boldsymbol{\omega}_k(\boldsymbol{x},t) = \boldsymbol{\gamma}_k \int_{-1}^{1} \delta\big(\boldsymbol{x}-(\boldsymbol{x}_k+s\boldsymbol{h}_k)\big)ds \tag{4}$$

$\boldsymbol{x}_k = \boldsymbol{x}_k(t)$ denotes the k-th fragmenton's marker position (the middle point of $2\boldsymbol{h}_k$); $\boldsymbol{\gamma}_k = \boldsymbol{\gamma}_k(t)$ is intensity (circulation); all the three parameters $\boldsymbol{x}_k, \boldsymbol{\gamma}_k, \boldsymbol{h}_k$ can change in time. $\boldsymbol{\gamma}_k$ is chosen to be collinear with $\boldsymbol{h}_k$, so it is convenient to write it as

$$\boldsymbol{\gamma}_k = \gamma_k \boldsymbol{h}_k, \tag{5}$$

where γ_k is a scalar weight coefficient that describes the intensity value with respect to the fragmenton length.

Taking the Bio-Savart integral of (4) one can find the velocity field, induced by a single fragmenton, placed into point $\boldsymbol{x}_k$ (see fig. 1)

$$\boldsymbol{V}_k = \frac{\gamma_k}{4\pi} \frac{\boldsymbol{h}_k \times \boldsymbol{s}_0}{|\boldsymbol{h}_k \times \boldsymbol{s}_0|^2} \left[\left(\frac{\boldsymbol{s}_2}{|\boldsymbol{s}_2|} - \frac{\boldsymbol{s}_1}{|\boldsymbol{s}_1|} \right) \cdot \boldsymbol{h}_k \right] \tag{6}$$

[1] Using the Helmholtz theorem vorton can be complemented to become solenoidal. Such basis function got the name "Novikov's vorton" [12]

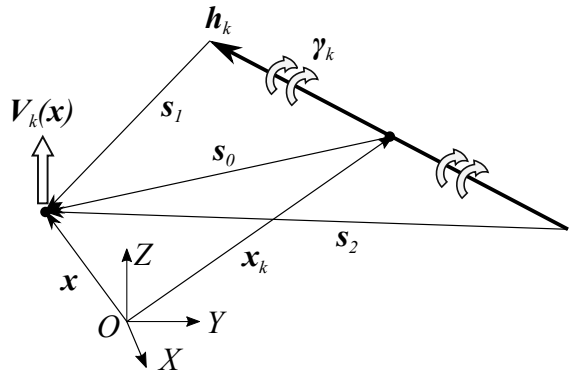

Fig. 1 Fragmenton model

Substitution of (4) into (2) and then into the vorticity evolution equation for ideal fluid ((1) with $\nu = 0$) allows to rewrite the original equation into the system of ODEs of fragmentons' parameters $\boldsymbol{x}_k$, $\boldsymbol{h}_k$ and γ_k [13]

$$\begin{cases} \dfrac{d\boldsymbol{x}_k}{dt} = \boldsymbol{V}(\boldsymbol{x}_k), \\ \dfrac{d\boldsymbol{h}_k}{dt} = \boldsymbol{h}_k \cdot \nabla \boldsymbol{V}(\boldsymbol{x}_k), \\ \dfrac{d\gamma_k}{dt} = 0. \end{cases} \tag{7}$$

Analysis of (7) shows that as in classical particle methods, the markers $\boldsymbol{x}_k$ follow the velocity field. However, the fragmenton orientation vector $\boldsymbol{h}_k$ can change its length and direction. $\boldsymbol{V}(\boldsymbol{x})$ is the velocity field, reconstructed as the superposition of (6); $\nabla \boldsymbol{V}(\boldsymbol{x}_k)$ is the velocity gradient tensor at point $\boldsymbol{x}_k$, it acts as deformation operator for $\boldsymbol{h}_k$. The explicit form of $\nabla \boldsymbol{V}(\boldsymbol{x})$ can be found in [13].

It should also be noted, that the scalar intensities γ_k of the vortex elements stay constant over time for ideal fluid ($\nu = 0$). If we consider a viscous fluid with the PSE or DVM-PSE scheme for the diffusion term $\nu\Delta\boldsymbol{\omega}$, it will not be the case anymore. Fragmenton approximation of the initial vorticity $\boldsymbol{\omega}_0(\boldsymbol{x})$ gives the initial data for this ODE system):

$$\begin{cases} \boldsymbol{x}_k(0) = \boldsymbol{x}_{0k}, \\ \boldsymbol{h}_k(0) = \boldsymbol{h}_{0k}, \\ \gamma_k(0) = \gamma_{0k}. \end{cases} \tag{8}$$

3 Particle Strength Exchange

Vorticity evolution equation for viscous fluid has the diffusion term $\nu\Delta\boldsymbol{\omega}$ that need a special treatment. The method was suggested and extensively analyzed by Degond & Mas-Gallic (1989) [7] as the mean to solve the advection-diffusion equations with the particle method as an alternative to splitting algorithm and the "random-walk" approach for diffusion [14].

PSE basically consists in approximation of the diffusion term $\nu\Delta\phi$ with the integral operator of the form

$$Q^\varepsilon(\phi) = \frac{\nu}{\varepsilon^2} \int_{\mathbb{R}^3} \eta_\varepsilon(\boldsymbol{x}-\boldsymbol{y})(\phi(\boldsymbol{y},t) - \phi(\boldsymbol{x},t))dy, \tag{9}$$

where $\eta_\varepsilon(\boldsymbol{x}) = \frac{1}{\varepsilon^3}\eta\left(\frac{\boldsymbol{x}}{\varepsilon}\right)$; $\eta(\boldsymbol{x}) \in L^1(\mathbb{R}^3)$ is called kernel function and ε is a cut-off parameter. Kernel function must satisfy several moment conditions in order to make $Q^\varepsilon(\phi)$ converge towards $\nu\Delta\phi$ in certain norms when $\varepsilon \to 0$. Details on the kernel function choice can be found in [7].

Consider an advection-diffusion equation

$$\frac{\partial \phi}{\partial t} + \nabla \cdot (\boldsymbol{V}\phi) = \nu\Delta\phi, \tag{10}$$

where $\boldsymbol{V} = \boldsymbol{V}(\boldsymbol{x},t)$ is a known vector field, ν – diffusion coefficient, $\phi = \phi(\boldsymbol{x},t)$ – unknown scalar function.

Here we want to show the particle method approach combined with the PSE approximation of the viscosity term $\nu\Delta\phi$. To do this consider the particle approximation ϕ_N of the field ϕ

$$\phi_N(\boldsymbol{x},t) = \sum_{k=1}^{N} \alpha_k \delta(\boldsymbol{x} - \boldsymbol{x}_k), \tag{11}$$

Substituting the (9) and (11) into (10) we get

$$\begin{cases} \dfrac{d\boldsymbol{x}_k}{dt} = \boldsymbol{V}(\boldsymbol{x}_k) \\ \dfrac{d\alpha_k}{dt} = \dfrac{\nu}{\varepsilon^2} \displaystyle\sum_{q=1}^{N} \eta_\varepsilon(\boldsymbol{x}_q - \boldsymbol{x}_k)\left(\phi(\boldsymbol{x}_q)\sigma_q - \phi(\boldsymbol{x}_k)\sigma_k\right) \end{cases} \tag{12}$$

where the PSE-integral is 'compensated' with the Dirac δ-functions. The particles follow the given field $\boldsymbol{V}$ that can be interpreted as velocity.

We perform, basically, the same procedure for the complete vorticity evolution equation (1) and apply there VE- and PSE-approximation. Omitting the calculations we come to the following ODEs (full derivations can be found in [15]):

$$\begin{cases} \dfrac{d\boldsymbol{x}_k}{dt} = \boldsymbol{V}(\boldsymbol{x}_k), \\ \dfrac{d\boldsymbol{h}_k}{dt} = \boldsymbol{h}_k \cdot \nabla \boldsymbol{V}(\boldsymbol{x}_k), \\ \dfrac{d\boldsymbol{\gamma}_k}{dt} = \boldsymbol{h}_k \cdot \nabla \boldsymbol{V}(\boldsymbol{x}_k) + \dfrac{\nu}{\varepsilon^2} \sum\limits_{q=1}^{N} G_{kq}(\boldsymbol{\gamma}_q \sigma_k - \boldsymbol{\gamma}_k \sigma_q). \end{cases} \tag{13}$$

here σ_k is the 'weight' of the k-th VE, which has a physical meaning of volume of space, occupied by one fragmenton. σ_k stay constant in time. G_{kq} denotes the exchange coefficient between k-th and q-th fragmentons, which depends on their length and mutual orientation.

$$G_{kq} = \int_{-1}^{1}\int_{-1}^{1} \eta_\varepsilon(x_k + \tau \boldsymbol{h}_k - \boldsymbol{x}_q - s\boldsymbol{h}_q) ds d\tau \tag{14}$$

4 Diffusion Velocity Method

Consider the advection-diffusion problem (10) given in section 3. One can rewrite the diffusion term $\nu\Delta\phi \equiv \nabla\cdot(\nu\nabla\phi)$ in the form $-\nabla\cdot(\boldsymbol{V}_d\phi)$, where $\boldsymbol{V}_d = -\nu\frac{\nabla\phi}{\phi}$ is called diffusion velocity, so that the equation (10) takes pure advective form

$$\frac{\partial\phi}{\partial t} + \nabla\cdot(\boldsymbol{V}_{eff}\phi) = 0, \tag{15}$$

where

$$\boldsymbol{V}_{eff} = \boldsymbol{V} + \boldsymbol{V}_d = \boldsymbol{V} - \nu\frac{\nabla\phi}{\phi}. \tag{16}$$

The introduced vector field $\boldsymbol{V}_{eff}$ nonlinearly depends on the unknown function ϕ. Before utilizing the particle approximation one should reformulate $\boldsymbol{V}_{eff}$ in the integral form. Consider a positive scalar function $\zeta(\boldsymbol{x})$, which satisfies the norming condition $\int_{\mathbb{R}^3}\zeta(\boldsymbol{x})d\boldsymbol{x} = 1$. Then, denoting $\zeta_\varepsilon(\boldsymbol{x}) = \frac{1}{\varepsilon^3}\zeta(\frac{\boldsymbol{x}}{\varepsilon})$ we approximate $\nabla\phi$ and ϕ as follows

$$\nabla\phi \approx \phi\star\nabla\zeta_\varepsilon, \tag{17}$$

$$\phi \approx \phi\star\zeta_\varepsilon, \tag{18}$$

where the star $\star$ denotes the convolution product in space. Using these approximations, we get smoothed diffusion velocity

$$\boldsymbol{V}_{d\varepsilon} = -\nu\frac{\phi\star\nabla\zeta_\varepsilon}{\phi\star\zeta_\varepsilon} \tag{19}$$

Substitution of (11) into $\boldsymbol{V}_{d\varepsilon}$ leads to the particle approximation of the diffusion velocity $\boldsymbol{V}^N_{d\varepsilon}$:

$$\boldsymbol{V}^N_{d\varepsilon}(\boldsymbol{x}) = -\nu\frac{\sum_{i=1}^N \alpha_i\nabla\zeta_\varepsilon(\boldsymbol{x}-\boldsymbol{x}_i)}{\sum_{i=1}^N \alpha_i\zeta_\varepsilon(\boldsymbol{x}-\boldsymbol{x}_i)} \tag{20}$$

Combining everything together we reformulate the original advection-diffusion equation (10) into a set of ODEs over the particle positions $\boldsymbol{x}_k$. Note that particle intensities α_k stay constant over time unlike in the PSE (13).

$$\frac{d\boldsymbol{x}_k}{dt} = \boldsymbol{V}(\boldsymbol{x}_k) + \boldsymbol{V}^N_{d\varepsilon}(\boldsymbol{x}_k) \tag{21}$$

One should admit that there exists no any known practical way to obtain the diffusion velocity for the vector diffusion term $\nu\Delta\boldsymbol{a}$, where $\boldsymbol{a}$ is arbitrary vector field, unless this field is either two-dimensional or axisymmetric. This is also true for the vortex methods, which successfully utilize the concept of diffusion velocity to simulate 2D and axisymmetric viscous flows [9].

5 Hybrid DVM-PSE approach

To overcome the mentioned issue the idea of a hybrid DVM-PSE scheme was suggested in [8, 10]. It involves splitting of the diffusion term $\nu\Delta\boldsymbol{\omega}$ into two parts, one of which can be reformulated via the diffusion velocity (DVM part), another part to be treated with the PSE method. It can be done in different ways, however, the most reasonable way to do this is to keep the DVM part maximal possible with respect to the PSE part. In what follows we will consider the splitting approach, suggested by Mycek (2016) [10], where the dominating DVM-part is found with the least squares method.

Consider the vorticity evolution equation written in the following form

$$\frac{\partial\boldsymbol{\omega}}{\partial t} + \nabla\cdot(\boldsymbol{V}\otimes\boldsymbol{\omega}) = (\boldsymbol{\omega}\cdot\nabla)\boldsymbol{V} + \nabla\cdot(\nu\nabla\boldsymbol{\omega}), \tag{22}$$

We decompose $\nu\nabla\boldsymbol{\omega}$ as the sum of two tensors

$$\nu\nabla\boldsymbol{\omega} = -\boldsymbol{V}_d \otimes \boldsymbol{\omega} + \hat{B}, \tag{23}$$

where $\boldsymbol{V}_d = \boldsymbol{V}_d(\boldsymbol{x},t)$ is the diffusion velocity field to be found, $\hat{B}$ is a tensor of a second order. We want to minimize $\hat{B} = \nu\nabla\boldsymbol{\omega} + \boldsymbol{V}_d \otimes \boldsymbol{\omega}$ with the relevant choice of the components V_{di} of $\boldsymbol{V}_d$ in a least squares manner as

$$\boldsymbol{V}_{di} = \arg\min_{x_d} \sum_{j=1}^{3} (\hat{A}_{ij} + x_i\boldsymbol{\omega}_j)^2 \tag{24}$$

where $\hat{A}$ denotes $\nu\nabla\boldsymbol{\omega}$.

Minimization of the objective function in (24) with respect to x_{di} gives the diffusion velocity of the form

$$\boldsymbol{V}_d = -\nu\frac{\nabla|\boldsymbol{\omega}|}{|\boldsymbol{\omega}|} \tag{25}$$

and tensor $\hat{B}$ (see [10] for details):

$$\hat{B} = \nu|\boldsymbol{\omega}|\left(\nabla\frac{\boldsymbol{\omega}}{|\boldsymbol{\omega}|}\right) \tag{26}$$

Substituting (25) and (26) into the vorticity evolution equation in (22) gives

$$\frac{\partial\boldsymbol{\omega}}{\partial t} + \nabla\cdot((\boldsymbol{V}+\boldsymbol{V}_d)\otimes\boldsymbol{\omega}) = (\boldsymbol{\omega}\cdot\nabla)\boldsymbol{V} + \nabla\cdot\hat{B}. \tag{27}$$

Here $\nabla\cdot\hat{B}$ is the part of the vorticity diffusion term $\nu\Delta\boldsymbol{\omega}$ that can be approximated with the PSE method.

We follow the DVM-PSE splitting concept and adapt both DVM and PSE schemes for the fragmenton model. First we approximate the diffusion velocity (25), using the cut-off function ζ_ε to smooth $\nabla|\boldsymbol{\omega}|$ and $|\boldsymbol{\omega}|$:

$$\boldsymbol{V}_d = -\nu\frac{\nabla|\boldsymbol{\omega}|}{|\boldsymbol{\omega}|} \approx -\nu\frac{|\boldsymbol{\omega}|\star\nabla\zeta_\varepsilon}{|\boldsymbol{\omega}|\star\zeta_\varepsilon} \tag{28}$$

Application of the quadrature rule for both numerator and denominator of smoothed $\boldsymbol{V}_d$ yields

$$\boldsymbol{V}_d \approx -\nu\frac{\sum_{k=1}^{N}|\boldsymbol{\gamma}_k|\int_{-1}^{1}\nabla\zeta_\varepsilon(\boldsymbol{x}-\boldsymbol{x}_k-s\boldsymbol{h}_k)ds}{\sum_{k=1}^{N}|\boldsymbol{\gamma}_k|\int_{-1}^{1}\zeta_\varepsilon(\boldsymbol{x}-\boldsymbol{x}_k-s\boldsymbol{h}_k)ds}, \tag{29}$$

where

$$|\boldsymbol{\gamma}_k| = \int_{S_k}|\boldsymbol{\omega}(\boldsymbol{x})|dS \approx |\boldsymbol{\omega}(\boldsymbol{x}_k)|S_k \tag{30}$$

The diffusion term $\nabla\cdot\hat{B}$ (26) in the DVM-PSE scheme has the form of a general diffusion operator $\nabla\cdot\big(D(\boldsymbol{x})\nabla\boldsymbol{a}(\boldsymbol{x})\big)$, appropriate for the PSE integral approximation. Following Lacombe and Mas-Gallic (1987) [8], one can write

$$\nabla\cdot\hat{B} \approx \frac{\nu}{2\varepsilon^2}\int_{\mathbb{R}^3}\eta_\varepsilon(\boldsymbol{x}-\boldsymbol{y})(|\boldsymbol{\omega}(\boldsymbol{x})|+|\boldsymbol{\omega}(\boldsymbol{y})|)\cdot \cdot\left[\frac{\boldsymbol{\omega}(\boldsymbol{y})}{|\boldsymbol{\omega}(\boldsymbol{y})|}-\frac{\boldsymbol{\omega}(\boldsymbol{x})}{|\boldsymbol{\omega}(\boldsymbol{x})|}\right]d\boldsymbol{y} \tag{31}$$

Combining the both DVM and PSE parts and applying the VE-approximation to (27) we get to the following ODE system over the fragmenton parameters $\boldsymbol{x}_k$, $\boldsymbol{h}_k$, σ_k and $\boldsymbol{\gamma}_k$:

$$\begin{cases} \dfrac{d\boldsymbol{x}_k}{dt} = \boldsymbol{V}_{eff}(\boldsymbol{x}_k), \\ \dfrac{d\boldsymbol{h}_k}{dt} = \boldsymbol{h}_k\cdot\nabla\boldsymbol{V}_{eff}(\boldsymbol{x}_k), \\ \dfrac{d\sigma_k}{dt} = (\nabla\cdot\boldsymbol{V}_d(\boldsymbol{x}_k))\sigma_k, \\ \dfrac{d\boldsymbol{\gamma}_k}{dt} = \boldsymbol{\gamma}_k\cdot\nabla\boldsymbol{V}(\boldsymbol{x}_k) + \dfrac{\nu}{2\varepsilon^2}\displaystyle\sum_{q=1}^{N}G_{kq}\left[\left(\frac{|\boldsymbol{h}_q|}{|\boldsymbol{h}_k|}\gamma_q\sigma_k + \right.\right. \\ \left.\left. + \dfrac{|\boldsymbol{h}_k|}{|\boldsymbol{h}_q|}\gamma_k\sigma_q\right)\left(\dfrac{\boldsymbol{h}_q}{|\boldsymbol{h}_q|}-\dfrac{\boldsymbol{h}_k}{|\boldsymbol{h}_k|}\right)\right] \end{cases} \tag{32}$$

where $\boldsymbol{V}_{eff} = \boldsymbol{V} + \boldsymbol{V}_d$.

6 Simulation examples

Here we give two representative examples of diffusion of two typical vortex structures: a rectilinear infinite vortex tube and a vortex ring with finite core radius. Both structures are rather regular and do not fully demonstrate the efficiency of the viscosity models, and we give them as the first step of investigation of the models.

Concerned problems have the distinctive feature that the adjacent fragmentons, which constitute both vortex structures, stay parallel to each other. This considerably simplifies the governing equations of all the viscosity models. In these

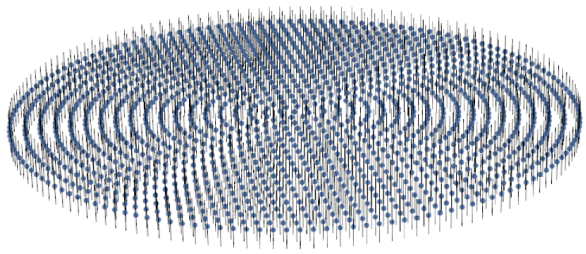

Fig. 2 Vortex tube section filled with fragmentons.

conditions one cannot even speak about the hybrid DVM-PSE model, because the PSE part of it is zero if $\boldsymbol{h}_k$ is parallel to $\boldsymbol{h}_q$ (32). So here we discuss the vortex tube diffusion, simulated with the PSE and DVM approaches, and the vortex ring with the DVM.

6.1 Vortex tube diffusion

Consider infinite rectilinear vortex tube of radius R, constructed with layers uniformly filled with fragmentons as shown on fig. 2. All the fragmentons have length $2\boldsymbol{h}$ and are oriented normally to the layer. In such configuration all the fragmentons stay parallel to each other and do not change their length. Practically it means that velocity gradient of such flow is always normal to $\boldsymbol{h}_k$ so that $\boldsymbol{h}_k \cdot \nabla \boldsymbol{V} \equiv 0$ in both models (13),(32).

It is known from theory that infinitely thin vorticity thread with initial circulation Γ_0 spreads in space and at time t has the following vorticity profile (in the plane, normal to thread)

$$\omega(r,t) = \frac{\Gamma_0}{4\pi\nu t} \exp\left(-\frac{r^2}{4\nu t}\right). \qquad (33)$$

Circulation at time t over the circle of radius R

$$\Gamma(t) = \Gamma_0 \left(1 - \exp\left(-\frac{R^2}{4\nu t}\right)\right) \qquad (34)$$

For the simulation we consider developed vortex tube with initial vorticity distribution $\omega(r,t_0)$, where t_0 is a moment of time, set as a parameter.

For both PSE and DVM simulations, the following parameters are chosen: Reynolds number $Re = 100$; viscosity $\nu = 0.01$; initial circulation

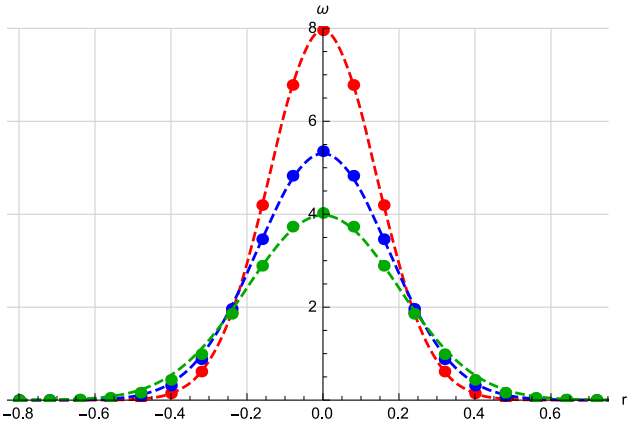

Fig. 3 Vortex tube vorticity profiles at the moments $t = 0$ (red), $t = 0.5$ (blue), $t = 1$ (green). Dots – PSE simulation; dashed line – theory

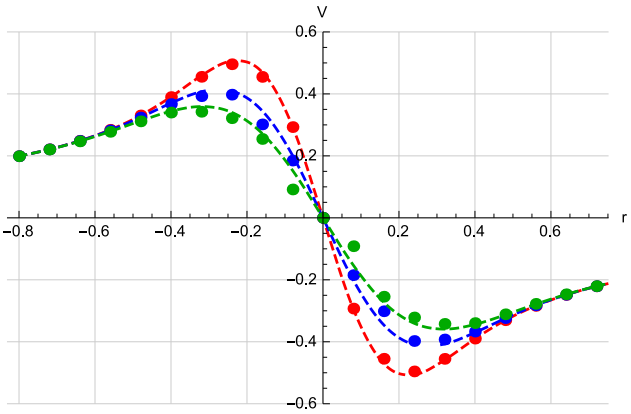

Fig. 4 Vortex tube velocity profiles at the moments $t = 0$ (red), $t = 0.5$ (blue), $t = 1$ (green). Dots – PSE simulation; dashed line – theory

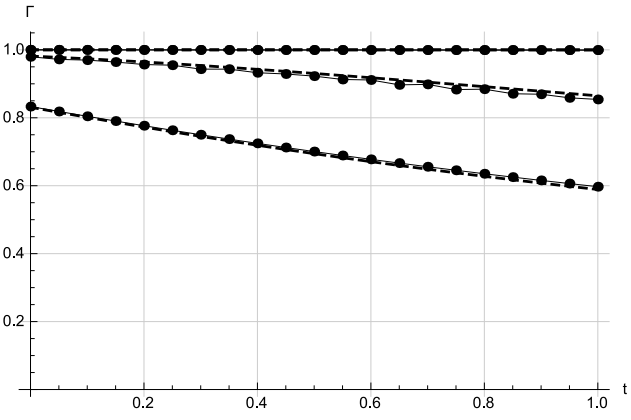

Fig. 5 Vortex tube circulations over circles of radii $R = 0.8$, $R = 0.4$ and $R = 0.27$. Dots – PSE simulation; dashed line – theory

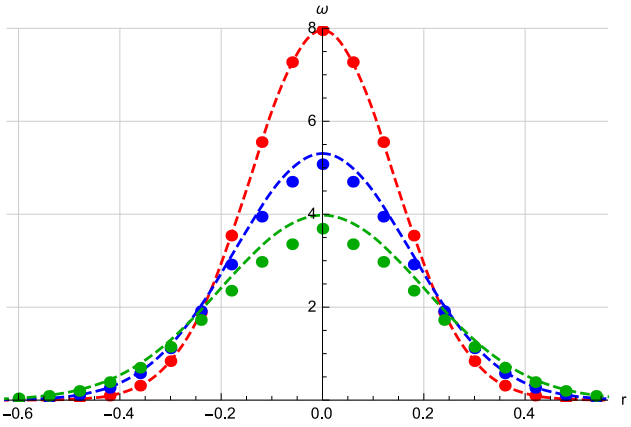

Fig. 6 Vortex tube vorticity profiles at the moments $t = 0$ (red), $t = 0.5$ (blue), $t = 1$ (green). Dots – DVM simulation; dashed line – theory

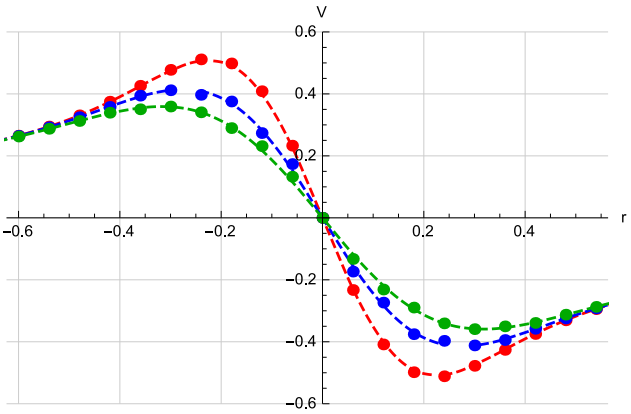

Fig. 7 Vortex tube velocity profiles at the moments $t = 0$ (red), $t = 0.5$ (blue), $t = 1$ (green). Dots – DVM simulation; dashed line – theory

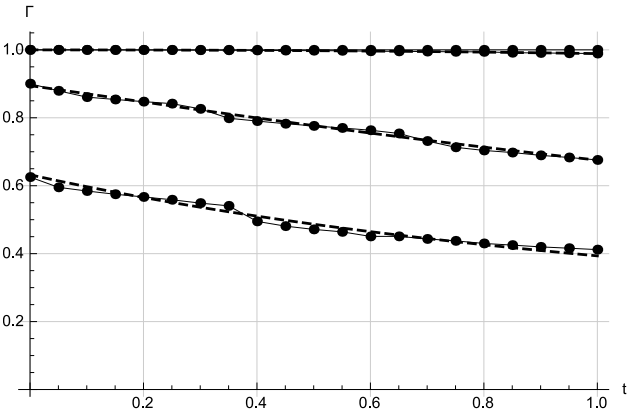

Fig. 8 Vortex tube circulations over circles of radii $R = 0.6$, $R = 0.3$ and $R = 0.2$. Dots – DVM simulation; dashed line – theory

$\Gamma_0 = 1$; fragmentons' length $2h = 0.1$ (with a total of 1259 VEs in a layer); number of considered layers (for viscosity modeling): 3; average distance between the VEs in layer $\Delta \approx 0.041$; cut-off parameter in the PSE model $\varepsilon = 0.041$; cut-off parameter in the DVM model $\varepsilon = 0.1$; time parameter $t_0 = 1$.

Equations (13), (32) are integrated up to time 1 either with the explicit 4th order Runge-Kutta method with fixed step $\Delta t = 0.01$ (DVM), or with the 1st order Euler with the same step (PSE).

Figures 3-4 show vorticity and velocity profiles of the vortex tube for times 0, 0.5 and 1. Dashed line denotes the analytical results, calculated with (33), (34), while the dots correspond to simulated results for the PSE approach. Figure 5 gives the circulation change in time over the circles of fixed radii 0.8, 0.4 and 0.27.

Figures 3-8 give the same graphs for the DVM simulation of the problem. Circulation graphs were obtained over the circles of radii 0.6, 0.3 and 0.2.

One can note small deviations of the dots' position from the analytical curves. This can be explained by close (or far) location of a fragmenton near the point of interest, while the calculated profiles in average show good correspondence. One can also notice some excessive diffusion in the DVM simulation, which can be corrected with the right choice of the parameter ε in diffusion velocity (28). This reveals the dependence of DVM over the model parameters, like inter-fragmenton distance and ε, which by all means must be bigger then the former.

6.2 Vortex ring diffusion

In this part we consider a test problem of vortex ring diffusion in viscous fluid. Though this problem does not have the exact solution, it can be solved analytically under the assumptions of a Stockes flow [16], where the viscous forces dominate over the convective forces. In particular, for vortex rings in a viscous fluid this model describes the ring's final development stage.

This 'Stokes' ring model has been intensively investigated theoretically by Kaplanski and Rudi

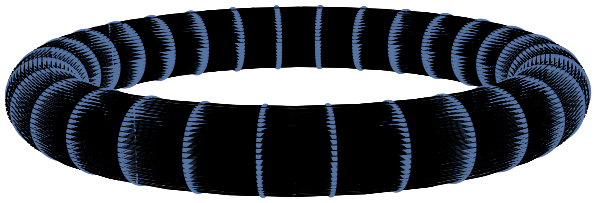

Fig. 9 Vortex ring model

[16] (we denote it as KR model). Comprehensive numerical analysis of vortex ring dynamics in a viscous flow and experiments [17] show that the model stays functional and give reliable results both for vortex ring formation stage and for its evolution stage, not necessarily with low Reynolds number. Therefore, we adopt this model and use it to compare with VEM simulation using the DVM-approach.

Consider an infinitely thin circular vortex filament of radius R_0 with the circulation Γ in a fluid with viscosity ν. Kaplanski [18] showed that in a Stokes flow vorticity field evolves in time and space as follows:

$$\omega = \frac{\Gamma R_0}{4\sqrt{\pi\nu^3 t^3}} \exp\left(-\frac{r^2+z^2+R_0^2}{4\nu t}\right) I_1\left(\frac{rR_0}{2\nu t}\right), \tag{35}$$

where r and z are the coordinates in a cylindrical frame that is translated with the ring so that the origin stays always in the ring center; $I_1(x)$ – modified Bessel function of the first kind.

As for the vortex tube, for the simulation we consider developed vortex ring with initial vorticity distribution $\omega(r,z,t_0)$, where t_0 is a moment of time, set as a parameter.

The figure 9 shows a vortex ring constructed with fragmentons. It consists of 30 sections of 225 fragmentons forming 8 circular layers in each section; circulation $\Gamma_0 = 1$; viscosity $\nu = 0.01$; Reynolds number $Re = \Gamma_0/\nu = 100$; ring radius $R = 1$; initial distance between adjacent fragmentons $\Delta \approx 0.011$; initial time parameter $t_0 = 0.1$; cut-off parameter in the DVM model $\varepsilon = 0.012$.

Equations (32) are integrated up to time 1 with the 1st order Euler method with fixed time step 0.01.

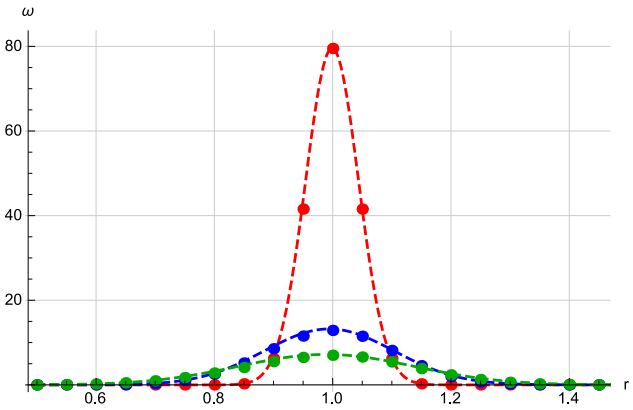

Fig. 10 Vortex ring vorticity profiles at the moments $t = 0$ (red), $t = 0.5$ (blue), $t = 1$ (green). Dots – DVM simulation; dashed line – theory

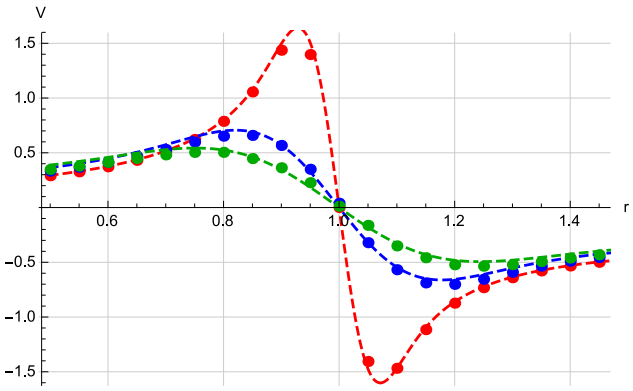

Fig. 11 Vortex ring velocity profiles at the moments $t = 0$ (red), $t = 0.5$ (blue), $t = 1$ (green). Dots – DVM simulation; dashed line – theory

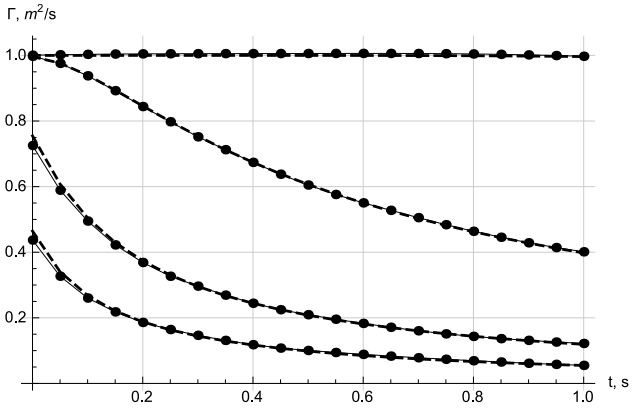

Fig. 12 Vortex ring circulations over circles of radii $R = 0.5$, $R = 0.15$, $R = 0.075$ and $R = 0.05$. Dots – DVM simulation; dashed line – theory

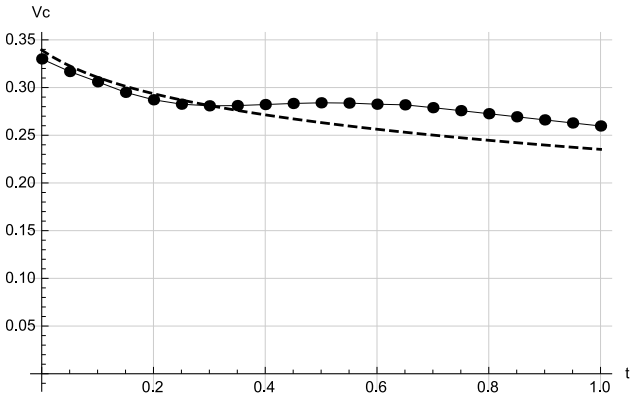

Fig. 13 Vortex ring self-translation velocity. Dots – DVM simulation; dashed line – theory

Figures 10-11 show vorticity and velocity profiles of the simulated vortex ring (dots) and analytical solution using the KR model (dashed line) for times 0, 0.5 and 1. Figure 12 gives the circulations evolution in time over the circles of radii 0.5, 0.15, 0.075 and 0.05. The circles' center moves with the central fragmenton since the vortex ring moves in fluid. Figure 13 shows the comparison of rings' displacement velocity with the one obtained from the KR model.

Comparison with the analytical results show small deviation profiles in time. KR model demonstrates more asymmetry in velocity profiles: the velocity closer to ring's center is higher than the further one. This effect is less revealed with the DVM-simulation. One also notice the deviation in the displacement velocity of the ring that starts at $t = 0.3$. It may be explained with the wrong methodology of ring's velocity determination in the simulation, where it is calculated as the velocity of the central fragmenton (in ring's section). The 'real' center of the ring's section may not always coincide with the same fragmenton.

7 Discussions

It this paper we gave general review of some approaches to model viscosity with the special vortex method based on fragmentons, that has showed good performance for ideal fluid simulations with respect to classical singular-point vortons. Here we show the outline and main results of adaption of PSE, DVM and DVM-PSE models for fragmentons. Each analyzed model ends with the ODEs over fragmenton parameters.

The examples discussed in the previous section show the correspondence to the theory. At the same time they reveal certain difficulties with the customization of the viscosity models, where the distance between fragmentons and the cut-off parameter ε may influence on the accuracy of the simulations. Although these two problems are very particular and by no means pretend to approve the reviewed viscosity models, they are important steps in further investigation of vortex methods and their application in viscous flows problems.

Before applying these models to more general cases, where the adjacent fragmentons are not parallel anymore, we cannot but mention the problem that reveals in VEM based on fragmentons. In viscous fluid fragmenton intensities $\boldsymbol{\gamma}_k$ and their direction $\boldsymbol{h}_k$ are not necessarily collinear as it was the case for ideal fluid. This may complicate the velocity reconstitution from a set of fragmentons. This is the question of further investigation.

References

[1] Cottet G-H., Koumoutsakos P. *Vortex Methods*. Cambridge: CUP, 2000.

[2] Kuzmina K.S., Marchevsky I.K., Ryatina E.P. Open Source Code for 2D Incompressible Flow Simulation by Using Meshless Lagrangian Vortex Methods. *Proceedings - 2017 Ivannikov ISPRAS Open Conference, ISPRAS 2017, 2018-January*, pp. 97-103.

[3] Kuzmina K.S., Marchevsky I.K., Moreva V.S. Vortex Sheet Intensity Computation in Incompressible Flow Simulation Around an Airfoil by Using Vortex Methods. *Mathematical Models and Computer Simulations*, Vol. 10 (3), pp. 276-287, 2018.

[4] Shcheglov G.A., Dergachev S.A. Hydrodynamic loads simulation for 3D bluff bodies by using the vortex loops based modification of the vortex particle method. *5th International Conference on Particle-Based Methods - Fun-*

damentals and Applications, PARTICLES 2017, pp. 725-731.

[5] Marchevsky I.K, Moreva V.S., Puzikova V.V. The efficiency comparison of the vortex element method and the immersed boundary method for numerical simulation of airfoil's hydroelastic oscillations. *VI International Conference on Computational Methods for Coupled Problems in Science and Engineering*, pp. 800-811, 2015.

[6] Kotsur O.S., Scheglov G.A., Leyland P. Verification of modelling of fluid structure interaction (FSI) problems based on experimental research of bluff body oscillations in fluids. *29th Congress of the International Council of the Aeronautical Sciences, ICAS 2014*, Paper ICAS2014-2.6.3-2014_0953.

[7] Degond P., Mas-Gallic S. The weighted particle method for convection-diffusion equations. Part1 and Part2. *Math.Comp.*, Vol. 53, No. 188, pp 485-525, 1989.

[8] Lacombe G., Mas-Gallic S. Presentation and Analysis of a Diffusion-Velocity Method. The linear case. *ESAIM: Proceedings*, Vol. 7, pp 225-233, 1999.

[9] Dynnikova G.Ya. Vortex Motion in Two-Dimensional Viscous Fluid Flows. *Fluid Dynamics*, Vol. 38, No. 5, pp 670-678, 2003.

[10] Mycek P., Pinon G., Germain G. and Rivoalen E. Formulation and analysis of a diffusion-velocity particle model for transport-dispersion equations. *Computational and Applied Mathematics*, Vol. 35, No. 2, pp 447-473, 2016.

[11] Beale J.T., Majda A. Vortex Methods. I: Convegence in Three Dimensions. *Mathematics of Computation*, Vol. 39, No. 159, pp 1-27, 1982.

[12] Novikov E. A. Generalized dynamics of three-dimensional vortex singularities (vortons). Zhurnal Eksperimentalnoi i Teoreticheskoi Fiziki. No. 8, pp 975-981, 1983.

[13] Marchevsky I., Shcheglov G. 3D vortex structures dynamics simulation using vortex fragmentons. *6th European Congress on Computational Methods in Applied Sciences and Engineering (ECCOMAS 2012)*, pp 5716-5735, 2012.

[14] Chorin A. Numerical study of slightly viscous flow. *Journal of Fluid Mechanics*. Vol. 57, No. 4, pp 785-796, 1973.

[15] Kotsur O.S., Shcheglov G.A. Implementation of the Particle Strength Exchange Method for Fragmentons to Account for Viscosity in Vortex Element Method. *Vestn. Mosk. Gos. Tekh. Univ. im. N.E. Baumana, Estestv. Nauki [Herald of the Bauman Moscow State Tech. Univ., Nat. Sci.]*, No. 3, pp. 48-67 (in Russ.), 2018. DOI: 10.18698/1812-3368-2018-3-48-67

[16] Kaplanski F.B., Rudi Y.A. A model for the formation of 'optimal' vortex ring taking into account viscosity. *Phys. Fluids*, Vol. 17, 087101, 2005.

[17] Danaila I., Helie J. Numerical simulation of the postformation evolution of a laminar vortex ring. *Physics of Fluids*, Vol. 20, 073602, 2008.

[18] Kaplanski F.B. On the diffusion of the vortex line. *Proc. of the Acad. of Sci. of the Est. SSR.*, Vol. 33, No. 3, pp 372-374, 1984.

8 Contact Author Email Address

Corresponding author: Oleg Kotsur
mailto: oskotsur@gmail.com

Copyright Statement